HHS Public Access

Author manuscript

Sci Total Environ. Author manuscript; available in PMC 2024 October 15.

Published in final edited form as:

Sci Total Environ. 2024 October 15; 947: 174478. doi:10.1016/j.scitotenv.2024.174478.

Engineering human midbrain organoid microphysiological systems to model prenatal PFOS exposure

Chunhui Tian[a], **Hongwei Cai**[a], **Zheng Ao**[a], **Longjun Gu**[a], **Xiang Li**[a], **Vivian C. Niu**[a,b], **Maria Bondesson**[a], **Mingxia Gu**[c,d], **Ken Mackie**[e], **Feng Guo**[a,*]

[a]Department of Intelligent Systems Engineering, Indiana University Bloomington, IN 47405, United States

[b]Bloomington High School South, Bloomington, IN 47401, United States

[c]Center for Stem Cell and Organoid Medicine (CuSTOM), Division of Pulmonary Biology, Division of Developmental Biology, Cincinnati Children's Hospital Medical Center, OH 45229, Cincinnati, United States

[d]University of Cincinnati School of Medicine, OH 45229, Cincinnati, United States

[e]Gill Center for Biomolecular Science, Department of Psychological and Brain Sciences, Indiana University Bloomington, IN 47405, United States

Abstract

Perfluorooctane sulfonate (PFOS), a class of synthetic chemicals detected in various environmental compartments, has been associated with dysfunctions of the human central nervous system (CNS). However, the underlying neurotoxicology of PFOS exposure is largely understudied due to the lack of relevant human models. Here, we report bioengineered human midbrain organoid microphysiological systems (hMO-MPSs) to recapitulate the response of a fetal human brain to multiple concurrent PFOS exposure conditions. Each hMO-MPS consists of an hMO on a fully 3D printed holder device with a perfusable organoid adhesion layer for enhancing air-liquid interface culturing. Leveraging the unique, simply-fabricated holder devices, hMO-MPSs are scalable, easy to use, and compatible with conventional well-plates, and allow easy transfer onto a multiple-electrode array (MEA) system for plug-and-play measurement of neural activity. Interestingly, the neural activity of hMO-MPSs initially increased and subsequently decreased by exposure to a concentration range of 0, 30, 100, to 300 μM of PFOS. Furthermore,

*Corresponding author. fengguo@iu.edu (F. Guo).

CRediT authorship contribution statement

Chunhui Tian: Writing – original draft, Investigation, Data curation. **Hongwei Cai:** Writing – review & editing, Validation, Methodology, Investigation. **Zheng Ao:** Writing – review & editing, Methodology, Data curation. **Longjun Gu:** Writing – review & editing, Methodology, Investigation. **Xiang Li:** Methodology, Investigation. **Vivian C. Niu:** Visualization, Data curation. **Maria Bondesson:** Writing – review & editing, Data curation. **Mingxia Gu:** Writing – review & editing, Data curation. **Ken Mackie:** Writing – review & editing, Data curation. **Feng Guo:** Writing – review & editing, Supervision, Funding acquisition, Conceptualization.

Declaration of competing interest

The authors declare that they have no known competing financial interests or personal relationships that could have appeared to influence the work reported in this paper.

Appendix A. Supplementary data

Supplementary data to this article can be found online at https://doi.org/10.1016/j.scitotenv.2024.174478.

PFOS exposure impaired neural development and promoted neuroinflammation in the engineered hMO-MPSs. Along with PFOS, our platform is broadly applicable for studies toxicology of various other environmental pollutants.

Graphical Abstract

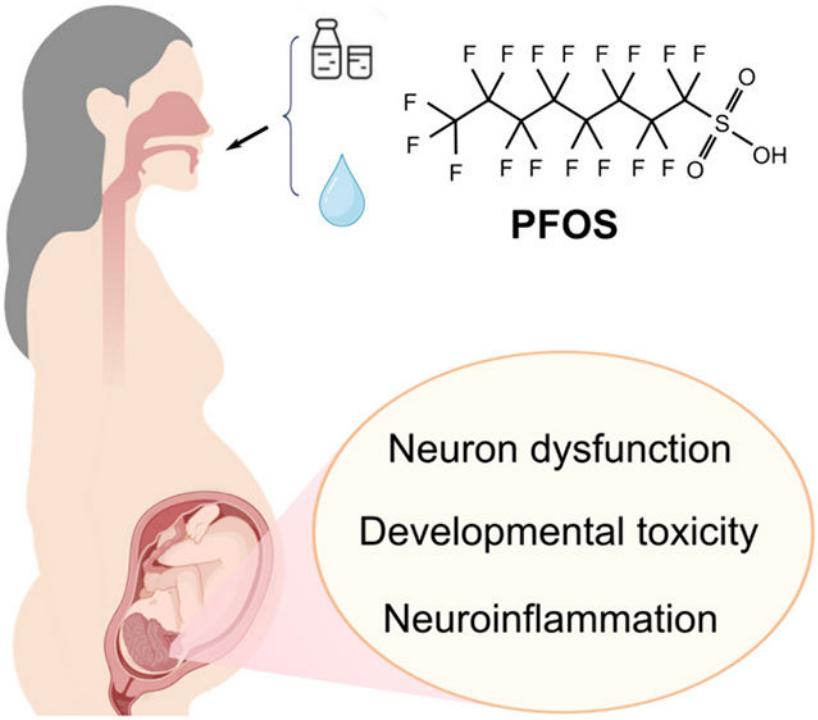

Keywords

PFOS; Toxicology; Brain organoids; Microphysiological systems; Brain development

1. Introduction

Perfluoroalkyl substances (PFAS) are a group of synthetic organic pollutants characterized by environmental bioaccumulation and persistence as well as high toxicity to human beings (Fábelová et al., 2023; De Silva et al., 2021; Glüge et al., 2020). PFAS are widely used in daily products such as food packaging, non-stick cookware, personal care products, textiles, paper, etc., and are detected in at least 45 % of U.S. tap water, putting people at risk of PFAS exposure (Wee and Aris, 2023; Smalling et al., 2023). Evidence of accumulation of PFAS in human brain tissue raises concerns about the health impact of PFAS on the brain (Pérez et al., 2013; Cao and Ng, 2021; Maestri et al., 2006). Among the many PFAS, perfluorooctane sulfonate (PFOS) stands out as particularly concerning due to its high toxicity and widespread detection in the global environment (Wee and Aris, 2023; Saikat et al., 2013). Substantial evidence shows that PFOS is detected in biological samples from people, including vulnerable pregnant women (Matilla-Santander et al., 2017; McAdam and Bell, 2023; Whitworth et al., 2012; Rovira et al., 2019). Because PFOS can cross the

placenta barrier actively or passively, it may adversely affect the developing embryo (Yao et al., 2023; Pan et al., 2017; Wang et al., 2019). Epidemiological studies provide evidence of a positive association between prenatal PFOS exposure and cognitive disorders in children (Vuong et al., 2021; Lenters et al., 2019). However, the precise developmental toxicity of PFOS is still largely understudied in humans.

Several models have been used to study the neurotoxicity of pollutants including PFOS. To date, two-dimensional (2D) in vitro neuron cultures illuminate that PFOS exposure generates reactive oxygen species (ROS), alters neuronal calcium load and morphology, and causes neuronal apoptosis (Liu et al., 2011; Pierozan and Karlsson, 2021; Li et al., 2017; Wang et al., 2015; Dusza et al., 2018; Fang et al., 2018). Studies in animal models reveal detrimental impacts of PFOS on the brain's dopaminergic system including reduced numbers of dopaminergic neurons and decreased levels of the dopamine neurotransmitter (Foguth et al., 2019; Kalyn et al., 2023; Grønnestad et al., 2021). These perturbations combined cause defective learning and memory in the brood (Grønnestad et al., 2021; Jantzen et al., 2016; Starnes et al., 2022). The 2D in vitro and animal models clearly demonstrate that PFOS exposure results in neurotoxicity. However, studies regarding the exact mechanisms of prenatal PFOS exposure in developing human brains are still limited. Whereas 2D in vitro models lack the intricate microenvironment of the brain and cannot faithfully replicate developmental processes, animal models do not fully recapitulate human biology and responses to PFOS exposure (Jucker, 2010; Kandratavicius et al., 2014). Thus, there is a tremendous need to develop three-dimensional (3D) human brain models to examine the effects of PFOS exposure on the developing human brain.

Human brain organoids, 3D brain-like tissues derived from human stem cells, recapitulate key physiological features of the developing human brain (Lancaster et al., 2013; PaŞca et al., 2015; Birey et al., 2017; Velasco et al., 2019; Pavon et al., 2024; Karzbrun et al., 2018). The human brain organoid models provide a promising solution to study the impact of toxicants on the developing fetal brain with the following advantages: (1) Current human brain organoids replicate the cell diversity of a developing human brain containing neurons, astrocytes, and neural progenitors (Di Lullo and Kriegstein, 2017; Karzbrun and Reiner, 2019); (2) Human brain organoids recapitulate structure and function of the developing human brain as well as its response to treatments (Trujillo et al., 2019; Pasca, 2018); and (3) Human brain organoids derived from human induced pluripotent stem cells (iPSCs) preserve an individual's genetic background and mutations (Birey et al., 2017; Qian et al., 2016; Iefremova et al., 2017). Different human brain organoids including cerebral organoids (Zhu et al., 2017; Bu et al., 2020; Huang et al., 2021; Bilinovich et al., 2021; Huang et al., 2024; Jiang et al., 2020; Liu et al., 2022), cortical organoids (Caporale et al., 2022; Adams et al., 2023; Chen et al., 2023), and forebrain organoids (Cao et al., 2023) have been applied to investigate the neurotoxicity of toxicants such as alcohol (Zhu et al., 2017; Adams et al., 2023), acrylamide (Bu et al., 2020), cadmium (Huang et al., 2021; Huang et al., 2024), diesel particulate matter (Bilinovich et al., 2021), endocrine disrupting chemicals (Caporale et al., 2022), nanoplastics (Chen et al., 2023), graphene oxide (Liu et al., 2022), and bisphenol A (Cao et al., 2023). However, current human brain organoids impose certain challenges including random cellular diversity and ratios, poor penetration of oxygen and nutrients, variable reproducibility, and low throughput. To address these

organoid challenges and promote neurotoxicity research, engineered organoid chips and microphysiological systems have been developed (Karzbrun et al., 2018; Wang et al., 2018a; Yin et al., 2018; Ao et al., 2020). By using a microfabricated compartment device, the Reiner group reported the first human brain organoids on a chip system for understanding the folding during the development of an embryonic human brain (Karzbrun et al., 2018). By employing microfabricated microfluidics, the Qin group developed a brain organoid-on-a-chip platform to study prenatal exposure to nicotine (Wang et al., 2018a). Moreover, they developed microfabricated pillar-array devices to culture human brain organoids for modeling impaired neurogenesis caused by cadmium (Yin et al., 2018). We have previously incorporated microfabricated devices with a human cerebral organoid protocol for a one-stop assembly of organoids to explore the neurotoxicity of prenatal cannabis exposure (Ao et al., 2020). Despite these recent advances in neurotoxicity research using brain organoid models, some limitations still exist including (1) The absence of a midbrain brain organoid model for examination of neurotoxicity on the dopaminergic system, which is crucial for memory, learning, attention, reward, and other cognitive functions (Wise, 2004); and (2) Inability to stably and reproducibly measure neural activity of brain organoids.

Here, we describe the development of innovative human midbrain organoid microphysiological systems (hMO-MPSs) to model the impact of prenatal PFOS exposure on human brain development. Our system boasts several unique features. Firstly, the utilization of hMOs within the system elucidates the impact of PFOS on the developing dopamine system in the human brain, an opportunity not possible in previous research. Secondly, the system supports the cultivation of many hMOs, facilitating the concurrent investigation of multiple conditions, such as different concentrations of PFOS important for the assessment of dose-toxicity relationships. Additionally, the incorporation of MEA plates in the system enables monitoring of neural activity in hMOs exposed to varying concentrations of PFOS, offering an intuitive view of the overall impact of toxicants on brain development. Utilizing this novel hMO-MPS, we simulate prenatal exposure to PFOS and demonstrate its adverse effects on human brain development.

2. Materials and methods

2.1. Preparation of PFOS solutions

Perfluorooctanesulfonic acid potassium salt (AK Scientific Inc) was dissolved in dimethylsulfoxide (DMSO) (Sigma) to a concentration of 600 mM and stored at 4 °C. The solution was placed in a sonicator (Branson) for five minutes to fully dissolve the perfluorooctanesulfonic acid potassium salt. The 600 mM stock solution was diluted to final concentrations with culture media before use.

2.2. Generation of human midbrain organoids

The human embryonic stem cell line used in this study was WA09 purchased from WiCell Institute. The application of the cell line strictly abides by the laws and regulations of WiCell Institute and Indiana University. The cells were cultured in Matrigel (Corning) pre-coated 6-well plates (Corning) with mTESR plus medium (Stemcell Technologies) changed three times a week. The cell culture plates were placed in an incubator which

maintained a constant temperature of 37 °C with 5% CO_2 (Thermo Fisher). ReLeSR (Stemcell Technologies) was used for the cell passage which occurred every five days. The hMOs were cultured according to a previously reported protocol (Jo et al., 2016). In brief, embryonic bodies (EBs) were generated by WA09 cells assembled in 96-well U bottom microplates (Corning) (around 9000 cells per well) and cultured under differentiation media with Matrigel embedding and orbital shaking (Jo et al., 2016).

2.3. Design and fabrication of holder devices

The device was first designed in AutoCAD software and then printed using 3D Printer (Phrozen) (Ao et al., 2022; Ao et al., 2021a; Cai et al., 2020a; Wu et al., 2020; Cai et al., 2023a). Design details of the device are shown in Fig. S1.

2.4. Culturing hMOs on holder devices

Organoids were loaded on the device after they were embedded in Matrigel. The seven-day Matrigel-embedded organoids were carefully aspirated with a pipette and placed on holder devices. The systems were cultured in ultra-low-attachment 24-well plates (Corning). The mesh of the device then presses the organoid underneath to increase the contact area of the organoid with the medium, which reduces hypoxia and necrosis. 600 μL culture medium was added into each well and was changed every other day to maintain midbrain organoids. The culture medium used for midbrain organoids was as described above.

2.5. Characterization of organoid neural activity

Two months old hMOs were used for electrical signal measurement using MEA plates (Axion) with electrodes in the center area (Cai et al., 2023b). The basal electrical signal was measured before PFOS addition. In the second set of experiments, organoids were cultured using Brain-Phys (Stemcell Technologies) in the absence or presence of 30, 100, or 300 μM PFOS. Culture media with 0.05 % DMSO was used for vehicle control treatments (0 μM PFOS). The measurements were conducted daily over one week, and each treatment group had six hMOs. The culture medium was changed daily to maintain the organoids during neural activity measurement.

2.6. Measurement and quantification of calcium levels

Cal-520 (Abcam) was used to measure calcium levels in hMOs. After seven days of PFOS treatment, hMOs (two months old) were transferred into fresh culture medium and incubated with Cal-520 at a dilution of 1:1000. After culturing in a 37 °C incubator with 5 % CO2 supply for 1 h, hMOs were washed three times with 1× phosphate-buffered saline (PBS) (Corning). Next, hMOs were transferred to a 96-well glass bottom plate (Thermo Fisher) with a transparent culture medium. There were five organoids in each group. The fluorescence intensity of each group was measured using an inverted fluorescence microscope (Olympus IX-83). The quantification of fluorescence intensity was performed with ImageJ (v 1.54f).

2.7. Measurement of dopamine

Dopamine concentrations of PFOS-exposed hMOs were measured using a Dopamine ELISA Kit (Abnova). After seven days of PFOS treatment, organoids (five months old) were transferred into a fresh culture medium with 200 μL medium per organoid. After 48 h of culturing in an incubator at 37 °C and 5 % CO2, 150 μL supernatant was collected with a pipette. After centrifuging at 300*g* for 10 min, 100 μL supernatant was diluted to 1000 μL for dopamine concentration measurements according to the manufacturer's protocol. Each ELISA assay sample utilized 100 μL of diluted supernatant, and the results were read by a Synergy H1 plate reader from BioTek.

2.8. Cryo-sectioning of organoids

For cryosectioning of hMOs, samples were initially washed twice with 1× PBS and fixed in 4 % paraformaldehyde (Thermo Fisher) in 1× PBS at 4 °C overnight. Following fixation, samples underwent cryo-protection by immersion in 30 % sucrose (Sigma) in 1× PBS (*w*/*v*) at 4 °C overnight. The prepared samples were then embedded in the O.C.T. compound (Fisher Scientific) in a cryomold (Sakura Finetek) and frozen on dry ice. Subsequently, the frozen samples were sectioned to a thickness of 30 μm using a cryostat (Leica) and collected on superfrost plus slides (VWR) (Ao et al., 2021b; Cai et al., 2021).

2.9. Immunofluorescence staining

Immunofluorescence staining was performed on cryosection slides. Initially, the slides underwent two 5-min washes with 1× PBS to eliminate O.C.T. compound residue. Subsequently, the slides were subjected to antigen retrieval (Thermo Fisher) via steam for 20 min. After cooling, they were rinsed with 1× PBS, followed by a 1-h incubation in blocking buffer (5 % normal serum (Jackson), 0.3 % Triton™ X-100 (Sigma) in 1× PBS) (Ao et al., 2021c). Primary antibodies, diluted in blocking buffer, were then applied to the slides and incubated overnight at 4 °C in a humidified, dark box. On the following day, slides underwent a 5-time, 10-min 1× PBS wash before a 2-h incubation with secondary antibodies (diluted in blocking buffer) in a humidified, dark box. The final steps involved a 3-time, 10-min 1× PBS wash and a 10-min incubation with DAPI (Thermo Fisher) diluted in 1× PBS. Detailed information on the antibodies used in the experiment is provided in Table S1. One month old organoids were used to stain FOXA2, ZO-1, Tuj1, and SOX2 expression. Two months old organoids were used to stain with antibodies towards TH, OTX2, GFAP, and MAP2.

2.10. qPCR analysis

To analyze the gene expression profile of hMOs, organoids were initially washed twice with 1× PBS, and RNA was extracted using the Quick RNA MicroPrep Kit (Zymo). The extracted RNA was promptly reverse-transcribed into complementary DNA using the qScript cDNA synthesis kit (Quantabio). Subsequently, cDNA was subjected to qPCR analysis using the SYBR Green real-time PCR master mix (Thermo Fisher). The detailed qPCR primer sequences are provided in Table S2 of the Supporting Information. Data analysis was performed using the ΔΔCt method, where the delta Ct value was calculated by subtracting the target gene Ct value in the organoids from the target gene Ct value in day 1

embryoid body (EB). The ΔCt was then normalized against the housekeeping gene GAPDH (Cai et al., 2020b). Each qPCR reaction was repeated three times.

2.11. Quantification of expression of neural progenitor cell, early-stage neurons, midbrain floor plate progenitor cells, and dopaminergic neurons

All the quantification was conducted based on immunofluorescence slides stained with corresponding antibodies (Table S1). Two staining slides per organoid were selected for quantification. The visualization was conducted using an inverted fluorescence microscope (Olympus IX-83). The quantification of cell ratio and fluorescence intensity was performed with ImageJ (v 1.54f). The averaged value obtained from two slides per organoid were presented as one data point in the results.

2.12. Quantification of astrocyte activation and neuron apoptosis

Astrocyte activation quantification was conducted based on immunofluorescence slides stained with an anti-GFAP antibody (Table S1). Neuron apoptosis was quantified with immunofluorescence slides stained with anto-NeuN and TUNEL assay. One staining slide per organoid was selected for quantification. The visualization was conducted using an inverted fluorescence microscope (Olympus IX-83). The quantification of fluorescence intensity and cell ratio was performed with ImageJ (v 1.54f). The value obtained from one slide per organoid were presented as one data point in the results.

2.13. Measurement and quantification of ROS

After seven days of PFOS treatment, the levels of ROS produced by hMOs (two months old) were measured using Total Reactive Oxygen Species (ROS) Assay Kit 520 nm (Life Technologies) according to the manufacturer's protocol. Briefly, the ROS Assay Stain solution in the kit was added to the PFOS-free culture medium of each organoid and co-cultured for one hour. Then the medium with ROS Assay Stain solution was aspirated and replaced with fresh media containing different concentrations of PFOS (30, 100, or 300 μM PFOS or vehicle control). There were five organoids in each group. The fluorescence intensity of each group was measured using an inverted fluorescent microscope (Olympus IX-83). The quantification of fluorescence intensity was performed with ImageJ (v 1.54f).

2.14. TUNEL staining

After immunofluorescence staining for NeuN, TUNEL staining was conducted on cryosection slides to visualize cell apoptosis using the In Situ Cell Death Detection Kit from Roche, following the provided protocol. In brief, the slides were initially fixed with a solution containing 4% paraformaldehyde in 1× PBS for 20 min at room temperature, followed by a 30-min wash with 1× PBS. Subsequently, the slides were incubated with Permeabilization solution (0.1 % Triton X–100, 0.1 % sodium citrate (Sigma)) on ice for 2 min. Following this, the slides were incubated with the TUNEL reaction mixture at 37 °C in a dark, humidified box for 1 h. Finally, the slides were embedded with antifade (Invitrogen) before visualization on a confocal microscope (Leica Stellaris 8).

2.15. Measurement and quantification of neurites in hMOs

For promoting the outgrowth of neurites, hMOs (two months old) were allowed to attach to fibronectin (Corning)-coated glass coverslips for 4 h in the presence of 10 μg/mL laminin (Sigma). The attached hMOs were subsequently incubated on coverslips for seven days under PFOS treatment and stained with Cal-520 (Abcam) to visualize neurons. Neurite outgrowth and coverage area were then captured using an inverted microscope (Olympus IX-83) and quantified by the ImageJ (v 1.54f).

2.16. Statistical analysis

Kolmogorov-Smirnov test and F test were used to evaluate normality and compare variances. The statistical comparisons of each group were performed by unpaired *t*-test with GraphPad Prism 8. The statistical significance of differences in values is denoted: $*p < 0.05$, $**p < 0.01$, $***p < 0.005$. $****p < 0.001$.

3. Results

3.1. Engineering human midbrain organoid microphysiological systems to model prenatal PFOS exposure

Toxic substances such as PFOS are pervasive in various environments integral to human existence, which has led to the presence of PFOS in pregnant women (Matilla-Santander et al., 2017). A prior study showed that PFOS can cross the placental barrier, potentially leading to harmful effects in the fetus, particularly in the developing brain (McAdam and Bell, 2023). Prenatal exposure to PFOS may cause several detrimental effects on the developing fetal brain (Fig. 1a). We engineered human midbrain organoid microphysiological systems (hMO-MPSs) to model PFOS exposure under multiple conditions in parallel (Fig. 1b). Each hMO-MPS consists of a hMO derived from human stem cells and a fully 3D-printed holder device with a perfusable layer. hMOs adhere onto the perfusable layer and are cultured in the holder device, which facilitates culturing in an air-liquid interface as well as mediates the formation of a flattened organoid shape. hMO-MPSs are cultured in conventional well plates in a concentration range of PFOS to investigate concentration-dependent toxicity. Due to the unique simply-fabricated holder devices, hMO-MPSs are easily transferred to the multiple-electrode array (MEA) system for plug-and-play measurement of neural activity. The flat organoid shape covers more MEA electrodes than round ones, allowing concurrent testing of multiple conditions of PFOS exposure.

We generated hMO-MPSs and characterized their biological composition, development, and maturation using cryosection and immunofluorescence staining (Fig. 1c). In one-month-old hMOs, two groups of staining highlight the organization of midbrain developmental structures, including the ventricular zone (VZ)-like area and sub-ventricular zone (SVZ)-like area. These include zonula occludens-1 (ZO-1) staining of tight junctions and forkhead box protein A2 (FOXA2) staining of midbrain floor plate progenitors, as well as SRY-box 2 (SOX2) staining of neural progenitors and class III beta-tubulin (Tuj1) staining of early-stage neurons. In two-month-old hMOs, tyrosine hydroxylase (TH), a canonical marker of dopaminergic neurons was detected in the organoids, indicating successful development of

these neurons. Along-side TH, orthodenticle homeobox 2 (OTX2) staining was detected, indicating the presence of midbrain intermediate progenitors. Furthermore, the presence of astrocytes as well as mature neurons was indicated by glial fibrillary acidic protein (GFAP) and microtubule-associated protein 2 (MAP2) staining, respectively.

3.2. PFOS impairs neural function

To investigate the effects of PFOS exposure on neural function, we first measured the neural activities of hMOs using a MEA system. Two-month-old organoids were utilized in the experiments since they are mature and exhibit robust neural activity at this stage (Jo et al., 2016). We characterized the neural activity of hMO after seven days of treatment with four concentrations of PFOS (0, 30, 100, and 300 μM), and obtained raster plots of neuronal depolarization for each concentration (Fig. 2a). We quantified the neural activity of hMOs along the time course in terms of mean firing rate, burst frequency, and synchrony index (Fig. 2b). We found that all doses of PFOS initially induced hyperexcitability in hMOs, followed by a gradual decrease in neural activity. The peak values of neural activity of hMOs treated with 30, 100, or 300 μM PFOS occurred at the third-, second-, and first-day post-exposure, respectively. The neural activities in the 30 μM PFOS-treated organoids dropped back to a slightly lower level compared to the vehicle control (0 μM) hMOs, whereas the neural activities in hMOs treated with 100 and 300 μM PFOS decreased rapidly after reaching a peak. hMOs treated with 300 μM PFOS had close to zero neural activity after seven days of PFOS exposure. These results demonstrated PFOS's initial and long-term excitotoxic effect on the neurons.

We also characterized the impact of PFOS on other neural functions of hMOs after seven days of exposure, including calcium levels and dopamine production. The fluorescence intensity of Cal-520 staining was used to characterize the levels of calcium, a crucial intracellular messenger in mammalian neurons (Fig. S2a). The results showed that the calcium levels in two-month-old hMOs decreased during the elevated PFOS exposure concentrations (Fig. S2b). The concentration of dopamine, a neurotransmitter playing key roles in pleasure, motivation, and learning (Klein et al., 2019), was measured using ELISA in five-month-old hMOs, due to their significant dopamine release at this stage (Fig. 2c). Similar to the calcium levels, the dopamine concentrations correlated inversely with the PFOS-exposure concentrations. Notably, only the 100 and 300 μM PFOS exposures resulted in significant decreases in calcium levels and dopamine concentrations, while 30 μM did not.

3.3. PFOS affects neural development

Since functional perturbations were observed in hMO-MPSs, especially at the high concentrations of PFOS treatment, we studied the impacts of 300 μM PFOS exposure on neural development. After 300 μM PFOS treatment for seven days, we characterized the changes of neural progenitor cells, early-stage neurons, midbrain floor plate progenitor cells in one-month-old hMOs, and dopaminergic neurons in two-month-old hMOs using immunofluorescence staining (Fig. 3a). We found a significant decrease of neural progenitor cells (SOX2) and differentiating early-stage neurons (Tuj1) in hMOs exposed to 300 μM PFOS compared to vehicle control, indicating PFOS's toxicity towards neurogenesis. Moreover, we found fewer midbrain floor plate progenitor cells (FOXA2) and dopaminergic

(TH) neurons in organoids treated with 300 μM PFOS, which is consistent with a previous report demonstrating that PFOS exposure reduces the number of dopaminergic neurons (Foguth et al., 2019). The above observations were confirmed by qPCR results (Fig. 3b). The relative gene expression of neural progenitor cell marker SOX2 and Paired Box protein 6 (PAX6), early-stage neuron maker Tuj1, midbrain layer marker nuclear receptor related 1 protein (NURR1), midbrain floor plate progenitor cells marker FOXA2, and dopaminergic neuron marker TH were all significantly decreased in organoids treated with 300 μM PFOS. Those findings indicate the detrimental impacts of high-concentration PFOS treatment on neural development.

3.4. PFOS induces neuroinflammation

Besides the impacts of PFOS on neural development, we also investigated its effect on neuroinflammation in hMO-MPSs. After seven days of treatment with no or 300 μM PFOS, we characterized the generation of ROS and astrocyte activation of hMO-MPSs with two-month-old hMOs using a ROS assay kit, immunofluorescence staining, and qPCR. The production of ROS, a key signal of the progression of inflammatory disorders (Kong et al., 2020), was quantified by fluorescence intensity after staining with a ROS indicator dye (Fig. 4a). We found that the generation of ROS significantly increased with 300 μM PFOS exposure (Fig. 4b). GFAP staining of astrocytes, a key regulator of inflammatory responses in the central nervous system, was conducted to detect astrocyte activation (Kang et al., 2014; Wang et al., 2018b) (Fig. 4c). PFOS exposure induced thicker and brighter astrocytes (Fig. 4c) and significantly higher fluorescence intensity of GFAP in hMOs compared to control, indicating possible astrocyte activation (Fig. 4d). This finding was confirmed by qPCR analysis showing that mRNA expression of GFAP increased in 300 μM PFOS-exposed hMOs (Fig. 4e). The elevated levels of ROS generation and astrocyte activation demonstrate PFOS's likely role in producing a neuroinflammatory state in the developing brain.

Finally, we measured neuron apoptosis and alteration of neurite morphology in two-month-old hMOs, which could be correlated with PFOS-induced neuroinflammation. hMOs were analyzed after seven days of exposure to no or 300 μM PFOS for apoptosis, neuronal structure, and calcium levels by immunofluorescence and Cal-520 staining. Co-staining for NeuN, which stains neural nuclei, and apoptosis stain by the TUNEL assay, indicated neuronal apoptosis (Fig. 5a). A clear vision of separated images was shown in Fig. S3. Quantification of the results revealed a higher percentage of TUNEL positive neurons in 300 μM PFOS-exposed organoids compared to control, indicating neuron apoptosis caused by PFOS exposure (Fig. 5b). The finding was confirmed by qPCR analysis for the expression of MAP2, which significantly decreased in PFOS-exposed hMOs (Fig. 5c). Furthermore, PFOS-induced perturbations of neurite morphology were explored with organoids attaching to glass bottom of plates to allow visualization of neurite outgrowth. Cal-520 was used to identify neurites (Fig. 5d). Both neurite density and coverage area were significantly decreased after 300 μM PFOS treatment (Fig. 5e).

4. Discussions

The neurotoxicity of PFOS has been studied using animal models, 2D in vitro cultures of animal cells, and 2D in vitro cultures of human cells. However, human brain organoids derived from human stem cells, especially human midbrain organoids, are not used for studying the neurotoxicity of PFOS yet, due to the challenges of using current organoids including high heterogeneity, poor reproducibility, low throughput, intensive manual handling, and limited perfusion of oxygen and nutrients. In this study, we anticipated the development of hMO-MPSs via the engineering innovations including 3D printed scaffolds for enhancing perfusion and integration of MEA measurement for electrophysiological response of PFOS in parallel. Compared to the 2D in vitro *cultures of human neurons, our* hMO-MPSs can provide 3D brain-like microenvironments. Compared to the animal model, our hMO-MPSs can recapitulate human biology but still lack some cell identities such as microglia, and oligodendrocytes and the capability of modeling the systemic responses to PFOS exposure.

The concentration, frequency, and duration of PFOS exposure vary in the real-world settings and cause profound effects on the population. PFOS is very stable with a half-life of about 5.4 years in humans (Lupton et al., 2015). With the various concentration and frequency of exposures, PFOS can be bioaccumulated in the human body. The plasma PFOS concentrations of general population in western countries have been detected ranging from 0.002 to 0.23 μM (Criswell et al., 2022; Gallo et al., 2012; Cheng et al., 2022). The PFOS concentrations of occupationally-exposed population in western countries have been observed ranging from 0.988 to 10 μM (Fromme et al., 2009; Lucas et al., 2023). Additionally, the PFOS concentrations of occupationally exposed populations in some urban areas can be as high as 25.9 μM (or 13 μg/mL) (Fromme et al., 2009). Especially the moderate concentrations (e.g., 100 to 2000 μM) of PFOS in the environment of utero and infant may cause metabolic disruption in infants and children (Andersen et al., 2010). Although the bio-concentration and bio-accumulation of constant PFOS exposure may have adverse effects on the development of human central nervous system, this study focused on the one-time high dose and acute exposure of PFOS on neurodevelopment. The findings indicated some important impacts of one-time, high-dose, and acute PFOS exposure on human brain development and function.

The prenatal PFOS exposure can lead to adverse neurodevelopmental outcomes during pregnancy and early childhood, including potential impaired cognitive function, behavior, and motor skills (Vuong et al., 2021; Spratlen et al., 2020; Goodman et al., 2023; Zhou et al., 2023). Moreover, some studies suggest the association of lower scores on cognitive and behavioral assessments in children with higher levels of prenatal PFOS (Lenters et al., 2019; Spratlen et al., 2020; Goodman et al., 2023). Tremendous interests have been attracted to study the impact of prenatal PFOS exposure on neural function and development. Our findings suggest that PFOS can disrupt cell signaling pathways of neurons including inducing oxidative stress, causing neuron apoptosis, promoting neural inflammation, and so on. Moreover, our findings also show that PFOS can affect neural function and neurotransmitter systems including changing neural activity, reducing dopamine concentration., These adverse effects of PFOS can lead to deficits in learning,

memory, and other cognitive functions in the developing human brain. Understanding these mechanisms is crucial for developing strategies to mitigate the harmful effects of PFOS on brain health.

5. Conclusions

To conclude, we present innovative hMO-MPSs as a model system to probe the effects of prenatal exposure to PFOS, a prevalent environmental pollutant with global distribution and significant epidemic impact. These hMO-MPSs are scalable, easy to use, and compatible with conventional well plates, as well as allowing easy transfer onto a MEA system and plug-and-play measurement of neural activity to different concentrations of PFOS. Additionally, we applied neural functional, anatomical, and molecular tests to evaluate the neurotoxicity of PFOS. Our findings highlight the adverse effects of PFOS on neural function and development, indicating increased ROS generation, possible astrocyte activation, neuronal apoptosis, and alterations in neurite morphology. Our findings provide valuable insights into the impact of PFOS on human brain function and development. Thus, our platforms have promising potential for wide-ranging applications in modeling the effects of pollutants on functional neural disorders and performing developmental toxicology studies of environmental toxins.

Supplementary Material

Refer to Web version on PubMed Central for supplementary material.

Acknowledgments

F.G. wants to acknowledge the support from the National Institutes of Health Awards (DP2AI160242 and U01DA056242). The authors also acknowledge the Indiana University Imaging Center (NIH1-S10OD024988-01).

Data availability

Data will be made available on request.

References

Adams JW, Negraes PD, Truong J, Tran T, Szeto RA, Guerra BS, Herai RH, Teodorof-Diedrich C, Spector SA, Del Campo M, 2023. Impact of alcohol exposure on neural development and network formation in human cortical organoids. Mol. Psychiatry 28 (4), 1571–1584. [PubMed: 36385168]

Andersen CS, Fei CY, Gamborg M, Nohr EA, Sorensen TIA, Olsen J, 2010. Prenatal exposures to Perfluorinated chemicals and anthropometric measures in infancy. Am. J. Epidemiol 172 (11), 1230–1237. 10.1093/aje/kwq289. [PubMed: 20940176]

Ao Z, Cai H, Havert DJ, Wu Z, Gong Z, Beggs JM, Mackie K, Guo F, 2020. One-stop microfluidic assembly of human brain organoids to model prenatal cannabis exposure. Anal. Chem 92 (6), 4630–4638. [PubMed: 32070103]

Ao Z, Cai H, Wu Z, Song S, Karahan H, Kim B, Lu H-C, Kim J, Mackie K, Guo F, 2021a. Tubular human brain organoids to model microglia-mediated neuroinflammation. Lab Chip 21 (14), 2751–2762. [PubMed: 34021557]

Ao Z, Cai H, Wu Z, Ott J, Wang H, Mackie K, Guo F, 2021b. Controllable fusion of human brain organoids using acoustofluidics. Lab Chip 21 (4), 688–699. [PubMed: 33514983]

Ao Z, Cai H, Wu Z, Krzesniak J, Tian C, Lai YY, Mackie K, Guo F, 2021c. Human spinal organoid-on-a-chip to model nociceptive circuitry for pain therapeutics discovery. Anal. Chem 94 (2), 1365–1372. [PubMed: 34928595]

Ao Z, Song S, Tian C, Cai H, Li X, Miao Y, Wu Z, Krzesniak J, Ning B, Gu M, 2022 Understanding immune-driven brain aging by human brain organoid microphysiological analysis platform. Adv. Sci 9 (27), 2200475.

Bilinovich SM, Uhl KL, Lewis K, Soehnlen X, Williams M, Vogt D, Prokop JW, Campbell DB, 2021. Integrated RNA sequencing reveals epigenetic impacts of diesel particulate matter exposure in human cerebral organoids. Dev. Neurosci 42 (5–6), 195–207.

Birey F, Andersen J, Makinson CD, Islam S, Wei W, Huber N, Fan HC, Metzler KRC, Panagiotakos G, Thom N, 2017. Assembly of functionally integrated human forebrain spheroids. Nature 545 (7652), 54–59. [PubMed: 28445465]

Bu Q, Huang Y, Li M, Dai Y, Fang X, Chen K, Liu Q, Xue A, Zhong K, Huang Y, 2020. Acrylamide exposure represses neuronal differentiation, induces cell apoptosis and promotes tau hyperphosphorylation in hESC-derived 3D cerebral organoids. Food Chem. Toxicol 144, 111643. [PubMed: 32763439]

Cai H, Wu Z, Ao Z, Nunez A, Chen B, Jiang L, Bondesson M, Guo F, 2020a. Trapping cell spheroids and organoids using digital acoustofluidics. Biofabrication 12 (3), 035025. [PubMed: 32438350]

Cai H, Ao Z, Hu L, Moon Y, Wu Z, Lu H-C, Kim J, Guo F, 2020b. Acoustofluidic assembly of 3D neurospheroids to model Alzheimer's disease. Analyst 145 (19), 6243–6253. [PubMed: 32840509]

Cai H, Ao Z, Wu Z, Song S, Mackie K, Guo F, 2021. Intelligent acoustofluidics enabled mini-bioreactors for human brain organoids. Lab Chip 21 (11), 2194–2205. [PubMed: 33955446]

Cai H, Ao Z, Tian C, Wu Z, Liu H, Tchieu J, Gu M, Mackie K, Guo F, 2023a. Brain organoid reservoir computing for artificial intelligence. Nature Electronics 6 (12), 1032–1039.

Cai H, Ao Z, Tian C, Wu Z, Kaurich C, Chen Z, Gu M, Hohmann AG, Mackie K, Guo F, 2023b. Engineering human spinal microphysiological systems to model opioid-induced tolerance. Bioactive Materials 22, 482–490. [PubMed: 36330161]

Cao Y, Ng C, 2021. Absorption, distribution, and toxicity of per-and polyfluoroalkyl substances (PFAS) in the brain: a review. Environ. Sci.: Processes Impacts 23 (11), 1623–1640.

Cao Y, Hu D, Cai C, Zhou M, Dai P, Lai Q, Zhang L, Fan Y, Gao Z, 2023. Modeling early human cortical development and evaluating neurotoxicity with a forebrain organoid system. Environ. Pollut 337, 122624. [PubMed: 37757934]

Caporale N, Leemans M, Birgersson L, Germain P-L, Cheroni C, Borbély G, Engdahl E, Lindh C, Bressan RB, Cavallo F, 2022. From cohorts to molecules: adverse impacts of endocrine disrupting mixtures. Science 375 (6582), eabe8244. [PubMed: 35175820]

Chen S, Chen Y, Gao Y, Han B, Wang T, Dong H, Chen L, 2023. Toxic effects and mechanisms of nanoplastics on embryonic brain development using brain organoids model. Sci. Total Environ 904, 166913. [PubMed: 37689192]

Cheng X, Wei Y, Zhang Z, Wang F, He J, Wang R, Xu Y, Keerman M, Zhang S, Zhang Y, 2022. Plasma PFOA and PFOS levels, DNA methylation, and blood lipid levels: a pilot study. Environ. Sci. Technol 56 (23), 17039–17051. [PubMed: 36374530]

Criswell RL, Wang Y, Christensen B, Botelho JC, Calafat AM, Peterson LA, Huset CA, Karagas MR, Romano ME, 2022. Concentrations of per-and polyfluoroalkyl substances in paired maternal plasma and human milk in the New Hampshire birth cohort. Environ. Sci. Technol 57 (1), 463–472. [PubMed: 36574487]

De Silva AO, Armitage JM, Bruton TA, Dassuncao C, Heiger-Bernays W, Hu XC, Kärrman A, Kelly B, Ng C, Robuck A, 2021. PFAS exposure pathways for humans and wildlife: a synthesis of current knowledge and key gaps in understanding. Environ. Toxicol. Chem 40 (3), 631–657. [PubMed: 33201517]

Di Lullo E, Kriegstein AR, 2017. The use of brain organoids to investigate neural development and disease. Nat. Rev. Neurosci 18 (10), 573–584. [PubMed: 28878372]

Dusza HM, Cenijn PH, Kamstra JH, Westerink RH, Leonards PE, Hamers T, 2018. Effects of environmental pollutants on calcium release and uptake by rat cortical microsomes. Neurotoxicology 69, 266–277. [PubMed: 30056177]

Fábelová L, Beneito A, Casas M, Colles A, Dalsager L, Den Hond E, Dereumeaux C, Ferguson K, Gilles L, Govarts E, 2023. PFAS levels and exposure determinants in sensitive population groups. Chemosphere 313, 137530. [PubMed: 36509187]

Fang X, Wu C, Li H, Yuan W, Wang X, 2018. Elevation of intracellular calcium and oxidative stress is involved in perfluorononanoic acid–induced neurotoxicity. Toxicol. Ind. Health 34 (3), 139–145. [PubMed: 29187073]

Foguth RM, Flynn RW, de Perre C, Iacchetta M, Lee LS, Sepúlveda MS, Cannon JR, 2019. Developmental exposure to perfluorooctane sulfonate (PFOS) and perfluorooctanoic acid (PFOA) selectively decreases brain dopamine levels in northern leopard frogs. Toxicol. Appl. Pharmacol 377, 114623. [PubMed: 31195004]

Fromme H, Tittlemier SA, Völkel W, Wilhelm M, Twardella D, 2009. Perfluorinated compounds–exposure assessment for the general population in Western countries. Int. J. Hyg. Environ. Health 212 (3), 239–270. [PubMed: 18565792]

Gallo V, Leonardi G, Genser B, Lopez-Espinosa M-J, Frisbee SJ, Karlsson L, Ducatman AM, Fletcher T, 2012. Serum perfluorooctanoate (PFOA) and perfluorooctane sulfonate (PFOS) concentrations and liver function biomarkers in a population with elevated PFOA exposure. Environ. Health Perspect 120 (5), 655–660. [PubMed: 22289616]

Glüge J, Scheringer M, Cousins IT, DeWitt JC, Goldenman G, Herzke D, Lohmann R, Ng CA, Trier X, Wang Z, 2020. An overview of the uses of per-and polyfluoroalkyl substances (PFAS). Environ. Sci.: Processes Impacts 22 (12), 2345–2373.

Goodman CV, Till C, Green R, El-Sabbagh J, Arbuckle TE, Hornung R, Lanphear B, Seguin JR, Booij L, Fisher M, 2023. Prenatal exposure to legacy PFAS and neurodevelopment in preschool-aged Canadian children: the MIREC cohort. Neurotoxicol. Teratol 98, 107181. [PubMed: 37178772]

Grønnestad R, Johanson SM, Müller MH, Schlenk D, Tanabe P, Krøkje Å, Jaspers VL, Jenssen BM, Raeder EM, Lyche JL, 2021. Effects of an environmentally relevant PFAS mixture on dopamine and steroid hormone levels in exposed mice. Toxicol. Appl. Pharmacol 428, 115670. [PubMed: 34371090]

Huang Y, Dai Y, Li M, Guo L, Cao C, Huang Y, Ma R, Qiu S, Su X, Zhong K, 2021 Exposure to cadmium induces neuroinflammation and impairs ciliogenesis in hESC-derived 3D cerebral organoids. Sci. Total Environ 797, 149043. [PubMed: 34303983]

Huang Y, Guo X, Lu S, Chen Q, Wang Z, Lai L, Liu Q, Zhu X, Luo L, Li J, 2024. Long-term exposure to cadmium disrupts neurodevelopment in mature cerebral organoids. Sci. Total Environ 912, 168923. [PubMed: 38065485]

Iefremova V, Manikakis G, Krefft O, Jabali A, Weynans K, Wilkens R, Marsoner F, Brändi B, Müller F-J, Koch P, 2017. An organoid-based model of cortical development identifies non-cell-autonomous defects in Wnt signaling contributing to miller-Dieker syndrome. Cell Rep. 19 (1), 50–59. [PubMed: 28380362]

Jantzen CE, Annunziato KM, Cooper KR, 2016. Behavioral, morphometric, and gene expression effects in adult zebrafish (Danio rerio) embryonically exposed to PFOA, PFOS, and PFNA. Aquat. Toxicol 180, 123–130. [PubMed: 27710860]

Jiang Y, Gong H, Jiang S, She C, Cao Y, 2020. Multi-walled carbon nanotubes decrease neuronal NO synthase in 3D brain organoids. Sci. Total Environ. 748, 141384. [PubMed: 32823226]

Jo J, Xiao Y, Sun AX, Cukuroglu E, Tran H-D, Göke J, Tan ZY, Saw TY, Tan C-P, Lokman H, 2016. Midbrain-like organoids from human pluripotent stem cells contain functional dopaminergic and neuromelanin-producing neurons. Cell Stem Cell 19 (2), 248–257. [PubMed: 27476966]

Jucker M, 2010. The benefits and limitations of animal models for translational research in neurodegenerative diseases. Nat. Med 16 (11), 1210–1214. [PubMed: 21052075]

Kalyn M, Lee H, Curry J, Tu W, Ekker M, Mennigen JA, 2023. Effects of PFOS, F-53B and OBS on locomotor behaviour, the dopaminergic system and mitochondrial function in developing zebrafish (Danio rerio). Environ. Pollut 326, 121479. [PubMed: 36958660]

Kandratavicius L, Balista PA, Lopes-Aguiar C, Ruggiero RN, Umeoka EH, Garcia-Cairasco N, Bueno-Junior LS, Leite JP, 2014. Animal models of epilepsy: use and limitations. Neuropsychiatr. Dis. Treat 1693–1705. [PubMed: 25228809]

Kang W, Balordi F, Su N, Chen L, Fishell G, Hébert JM, 2014. Astrocyte activation is suppressed in both normal and injured brain by FGF signaling. Proc. Natl. Acad. Sci 111 (29), E2987–E2995. [PubMed: 25002516]

Karzbrun E, Reiner O, 2019. Brain organoids—a bottom-up approach for studying human neurodevelopment. Bioengineering 6 (1), 9. [PubMed: 30669275]

Karzbrun E, Kshirsagar A, Cohen SR, Hanna JH, Reiner O, 2018. Human brain organoids on a chip reveal the physics of folding. Nat. Phys 14 (5), 515–522. [PubMed: 29760764]

Klein MO, Battagello DS, Cardoso AR, Hauser DN, Bittencourt JC, Correa RG, 2019. Dopamine: functions, signaling, and association with neurological diseases. Cell. Mol. Neurobiol 39 (1), 31–59. [PubMed: 30446950]

Kong N, Ji X, Wang J, Sun X, Chen G, Fan T, Liang W, Zhang H, Xie A, Farokhzad OC, 2020. ROS-mediated selective killing effect of black phosphorus: mechanistic understanding and its guidance for safe biomedical applications. Nano Lett. 20 (5), 3943–3955. [PubMed: 32243175]

Lancaster MA, Renner M, Martin C-A, Wenzel D, Bicknell LS, Hurles ME, Homfray T, Penninger JM, Jackson AP, Knoblich JA, 2013. Cerebral organoids model human brain development and microcephaly. Nature 501 (7467), 373–379. [PubMed: 23995685]

Lenters V, Iszatt N, Forns J, Čechová E, Kočan A, Legler J, Leonards P, Stigum H, Eggesbø M, 2019. Early-life exposure to persistent organic pollutants (OCPs, PBDEs, PCBs, PFASs) and attention-deficit/hyperactivity disorder: a multi-pollutant analysis of a Norwegian birth cohort. Environ. Int 125, 33–42. [PubMed: 30703609]

Li Z, Liu Q, Liu C, Li C, Li Y, Li S, Liu X, Shao J, 2017. Evaluation of PFOS-mediated neurotoxicity in rat primary neurons and astrocytes cultured separately or in co-culture. Toxicol. In Vitro 38, 77–90. [PubMed: 27825932]

Liu X, Jin Y, Liu W, Wang F, Hao S, 2011. Possible mechanism of perfluorooctane sulfonate and perfluorooctanoate on the release of calcium ion from calcium stores in primary cultures of rat hippocampal neurons. Toxicol. In Vitro 25 (7), 1294–1301. [PubMed: 21575708]

Liu X, Yang C, Chen P, Zhang L, Cao Y, 2022. The uses of transcriptomics and lipidomics indicated that direct contact with graphene oxide altered lipid homeostasis through ER stress in 3D human brain organoids. Sci. Total Environ 849, 157815. [PubMed: 35931159]

Lucas K, Gaines LG, Paris-Davila T, Nylander-French LA, 2023. Occupational exposure and serum levels of per-and polyfluoroalkyl substances (PFAS): a review. Am. J. Ind. Med 66 (5), 379–392. [PubMed: 36573587]

Lupton SJ, Dearfield KL, Johnston JJ, Wagner S, Huwe JK, 2015. Perfluorooctane sulfonate plasma half-life determination and long-term tissue distribution in beef cattle (Bos taurus). J. Agric. Food Chem 63 (51), 10988–10994. 10.1021/acs.jafc.5b04565. [PubMed: 26684745]

Maestri L, Negri S, Ferrari M, Ghittori S, Fabris F, Danesino P, Imbriani M, 2006. Determination of perfluorooctanoic acid and perfluorooctanesulfonate in human tissues by liquid chromatography/single quadrupole mass spectrometry. Rapid Communications in Mass Spectrometry: An International Journal Devoted to the Rapid Dissemination of Up-to-the-Minute Research in Mass Spectrometry 20 (18), 2728–2734.

Matilla-Santander N, Valvi D, Lopez-Espinosa M-J, Manzano-Salgado CB, Ballester F, Ibarluzea J, Santa-Marina L, Schettgen T, Guxens M, Sunyer J, 2017. Exposure to perfluoroalkyl substances and metabolic outcomes in pregnant women: evidence from the Spanish INMA birth cohorts. Environ. Health Perspect 125 (11), 117004. [PubMed: 29135438]

McAdam J, Bell EM, 2023. Determinants of maternal and neonatal PFAS concentrations: a review. Environ. Health 22 (1), 1–33. [PubMed: 36600281]

Pan Y, Zhu Y, Zheng T, Cui Q, Buka SL, Zhang B, Guo Y, Xia W, Yeung LW, Li Y, 2017. Novel chlorinated polyfluorinated ether sulfonates and legacy per–/polyfluoroalkyl substances: placental transfer and relationship with serum albumin and glomerular filtration rate. Environ. Sci. Technol 51 (1), 634–644. [PubMed: 27931097]

Paşca AM, Sloan SA, Clarke LE, Tian Y, Makinson CD, Huber N, Kim CH, Park J-Y, O'rourke NA, Nguyen KD, 2015. Functional cortical neurons and astrocytes from human pluripotent stem cells in 3D culture. Nat. Methods 12 (7), 671–678. [PubMed: 26005811]

Pasca SP, 2018. The rise of three-dimensional human brain cultures. Nature 553 (7689), 437–445. [PubMed: 29364288]

Pavon N, Diep K, Yang F, Sebastian R, Martinez-Martin B, Ranjan R, Sun Y, Pak C, 2024. Patterning ganglionic eminences in developing human brain organoids using a morphogen-gradient-inducing device. Cell Reports Methods 4 (1).

Pérez F, Nadal M, Navarro-Ortega A, Fàbrega F, Domingo JL, Barceló D, Farré M, 2013. Accumulation of perfluoroalkyl substances in human tissues. Environ. Int 59, 354–362. [PubMed: 23892228]

Pierozan P, Karlsson O, 2021. Differential susceptibility of rat primary neurons and neural stem cells to PFOS and PFOA toxicity. Toxicol. Lett 349, 61–68. [PubMed: 34126183]

Qian X, Nguyen HN, Song MM, Hadiono C, Ogden SC, Hammack C, Yao B, Hamersky GR, Jacob F, Zhong C, 2016. Brain-region-specific organoids using mini-bioreactors for modeling ZIKV exposure. Cell 165 (5), 1238–1254. [PubMed: 27118425]

Rovira J, Martínez MÁ, Sharma RP, Espuis T, Nadal M, Kumar V, Costopoulou D, Vassiliadou I, Leondiadis L, Domingo JL, 2019. Prenatal exposure to PFOS and PFOA in a pregnant women cohort of Catalonia, Spain. Environmental research 175, 384–392. [PubMed: 31154228]

Saikat S, Kreis I, Davies B, Bridgman S, Kamanyire R, 2013. The impact of PFOS on health in the general population: a review. Environ. Sci.: Processes Impacts 15 (2), 329–335.

Smalling KL, Romanok KM, Bradley PM, Morriss MC, Gray JL, Kanagy LK, Gordon SE, Williams BM, Breitmeyer SE, Jones DK, 2023. Per-and polyfluoroalkyl substances (PFAS) in United States tapwater: comparison of underserved private-well and public-supply exposures and associated health implications. Environ. Int 108033. [PubMed: 37356308]

Spratlen MJ, Perera FP, Lederman SA, Rauh VA, Robinson M, Kannan K, Trasande L, Herbstman J, 2020. The association between prenatal exposure to perfluoroalkyl substances and childhood neurodevelopment. Environ. Pollut 263, 114444. [PubMed: 32272335]

Starnes HM, Rock KD, Jackson TW, Belcher SM, 2022. A critical review and meta-analysis of impacts of per-and polyfluorinated substances on the brain and behavior. Front. Toxicol 37.

Trujillo CA, Gao R, Negraes PD, Gu J, Buchanan J, Preissl S, Wang A, Wu W, Haddad GG, Chaim IA, 2019. Complex oscillatory waves emerging from cortical organoids model early human brain network development. Cell Stem Cell 25 (4), 558–569 (e557). [PubMed: 31474560]

Velasco S, Kedaigle AJ, Simmons SK, Nash A, Rocha M, Quadrato G, Paulsen B, Nguyen L, Adiconis X, Regev A, 2019. Individual brain organoids reproducibly form cell diversity of the human cerebral cortex. Nature 570 (7762), 523–527. [PubMed: 31168097]

Vuong AM, Webster GM, Yolton K, Calafat AM, Muckle G, Lanphear BP, Chen A, 2021. Prenatal exposure to per-and polyfluoroalkyl substances (PFAS) and neurobehavior in US children through 8 years of age: the HOME study. Environ. Res 195, 110825. [PubMed: 33545124]

Wang Y, Zhao H, Zhang Q, Liu W, Quan X, 2015. Perfluorooctane sulfonate induces apoptosis of hippocampal neurons in rat offspring associated with calcium overload. Toxicol. Res 4 (4), 931–938.

Wang Y, Wang L, Zhu Y, Qin J, 2018a. Human brain organoid-on-a-chip to model prenatal nicotine exposure. Lab Chip 18 (6), 851–860. [PubMed: 29437173]

Wang Y, Chen Y, Zhou Q, Xu J, Qian Q, Ni P, Qian Y, 2018b. Mild endoplasmic reticulum stress protects against lipopolysaccharide-induced astrocytic activation and blood-brain barrier hyperpermeability. Front. Cell. Neurosci 12, 222. [PubMed: 30104960]

Wang Y, Han W, Wang C, Zhou Y, Shi R, Bonefeld-Jørgensen EC, Yao Q, Yuan T, Gao Y, Zhang J, 2019. Efficiency of maternal-fetal transfer of perfluoroalkyl and polyfluoroalkyl substances. Environ. Sci. Pollut. Res 26, 2691–2698.

Wee SY, Aris AZ, 2023. Environmental impacts, exposure pathways, and health effects of PFOA and PFOS. Ecotoxicol. Environ. Saf 267, 115663. [PubMed: 37976959]

Whitworth KW, Haug LS, Baird DD, Becher G, Hoppin JA, Skjaerven R, Thomsen C, Eggesbo M, Travlos G, Wilson R, 2012. Perfluorinated compounds in relation to birth weight in the Norwegian Mother and Child Cohort Study. Am. J. Epidemiol 175 (12), 1209–1216. [PubMed: 22517810]

Wise RA, 2004. Dopamine, learning and motivation. Nat. Rev. Neurosci 5 (6), 483–494. [PubMed: 15152198]

Wu Z, Gong Z, Ao Z, Xu J, Cai H, Muhsen M, Heaps S, Bondesson M, Guo S, Guo F, 2020. Rapid microfluidic formation of uniform patient-derived breast tumor spheroids. ACS Appl. Bio Mater 3 (9), 6273–6283.

Yao H, Fu Y, Weng X, Zeng Z, Tan Y, Wu X, Zeng H, Yang Z, Li Y, Liang H, 2023 The association between prenatal per-and polyfluoroalkyl substances exposure and neurobehavioral problems in offspring: a meta-analysis. Int. J. Environ. Res. Public Health 20 (3), 1668. [PubMed: 36767045]

Yin F, Zhu Y, Wang Y, Qin J, 2018. Engineering brain organoids to probe impaired neurogenesis induced by cadmium. ACS Biomater Sci. Eng 4 (5), 1908–1915. [PubMed: 33445346]

Zhou Y, Li Q, Wang P, Li J, Zhao W, Zhang L, Wang H, Cheng Y, Shi H, Li J, 2023. Associations of prenatal PFAS exposure and early childhood neurodevelopment: evidence from the Shanghai maternal-child pairs cohort. Environ. Int 173, 107850. [PubMed: 36857906]

Zhu Y, Wang L, Yin F, Yu Y, Wang Y, Shepard MJ, Zhuang Z, Qin J, 2017. Probing impaired neurogenesis in human brain organoids exposed to alcohol. Integr. Biol 9 (12), 968–978.

HIGHLIGHTS

- Neurotoxicity of PFOS was first demonstrated using human midbrain organoids.
- Organoid neural activity increased and decreased to a PFOS concentration range.
- PFOS exposure impaired neurogenesis and promoted neuroinflammation in organoids.
- Our organoid system is scalable, easy to use, and appliable to various pollutants.

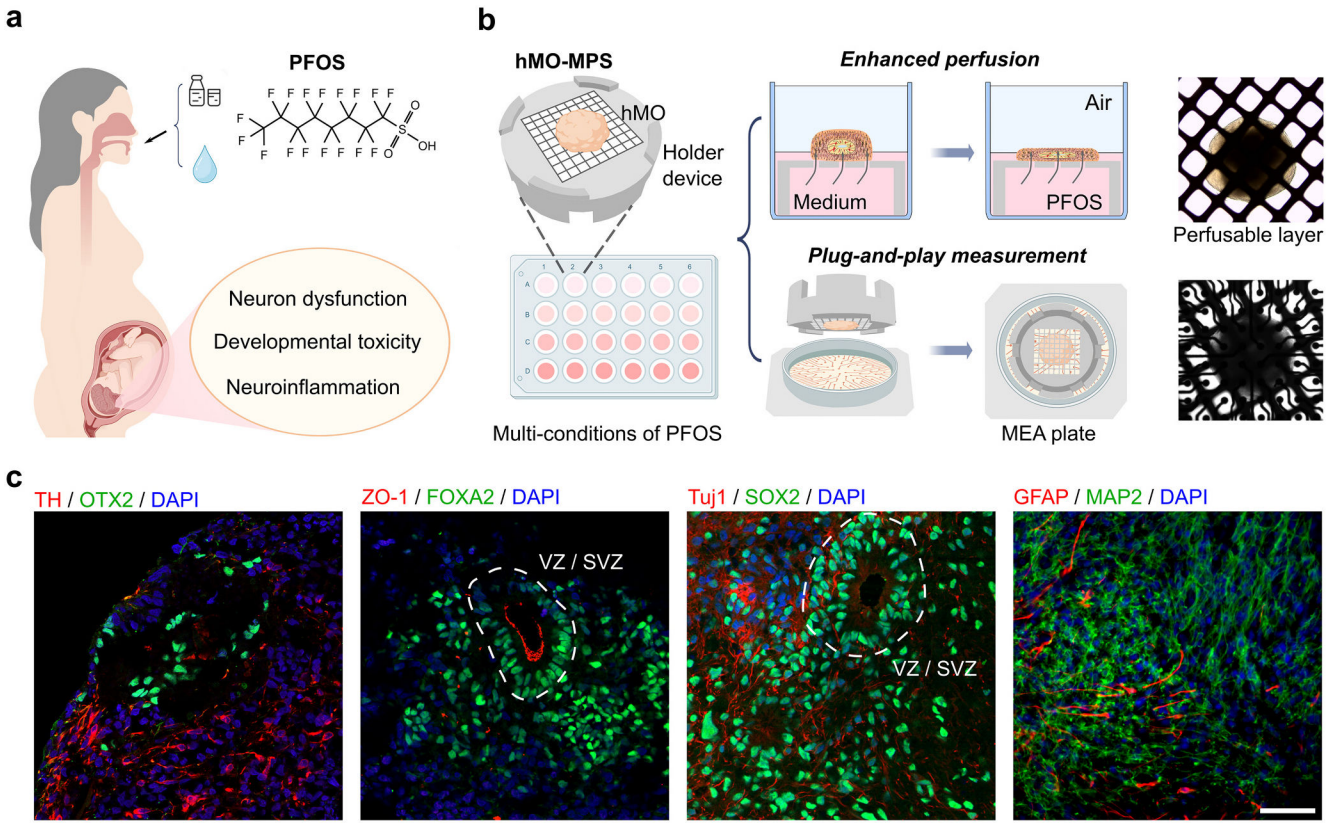

Fig. 1.

Human midbrain organoid microphysiological systems to model prenatal PFOS exposure. (a) Schematics of prenatal PFOS exposure and its effect on brain development. (b) Schematics of human midbrain organoid microphysiological systems (hMO-MPSs) to mode prenatal PFOS exposure. Inserted images of a hMO on the perfusable layer of the holder device (top), and hMO-MPS on a MEA plate (bottom). (c) Immunofluorescence staining showing cell types within one-month-old hMOs: midbrain floor plate progenitor cells (FOXA2), zonula occludens (ZO)-1, early-stage neurons (Tuj1), and neural progenitor cells (SOX2); within two-month-old hMOs: dopaminergic neurons (TH), intermediate progenitor cells (OTX2), astrocytes (GFAP), and mature neurons (MAP2). Scale bar: 50 μm.

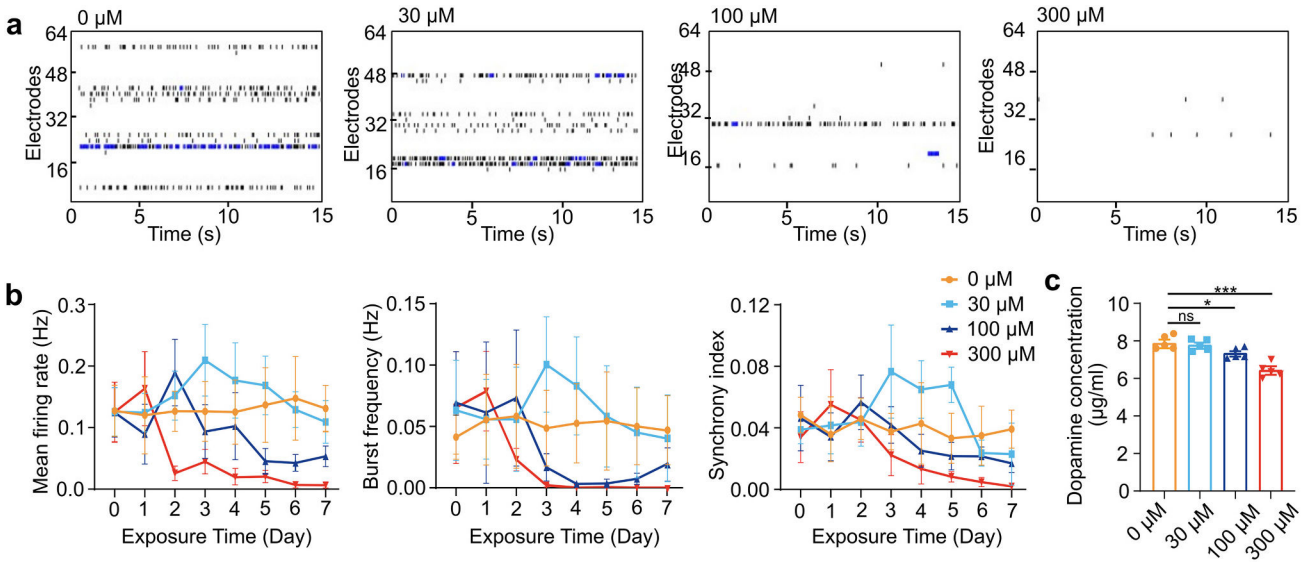

Fig. 2.

PFOS impairs neural activity and function. (a) Representative raster plots of spontaneous neuronal depolarizations of hMO-MPSs with two-month-old hMOs after exposure to different concentrations of PFOS for 7 days. (b) Changes of mean firing rate, burst frequency, and synchrony index during a 7-day exposure to control (vehicle, 0 μM PFOS) and PFOS at different concentrations (30, 100, and 300 μM) (mean ± s.e.m., $n = 6$ organoids, from 3 independent experiments). (c) Dopamine concentration changes of five-month-old hMOs after 7 days of exposure to increasing concentrations of PFOS (mean ± s.e.m., unpaired *t*-test, n = 5 organoids, from 3 independent experiments).

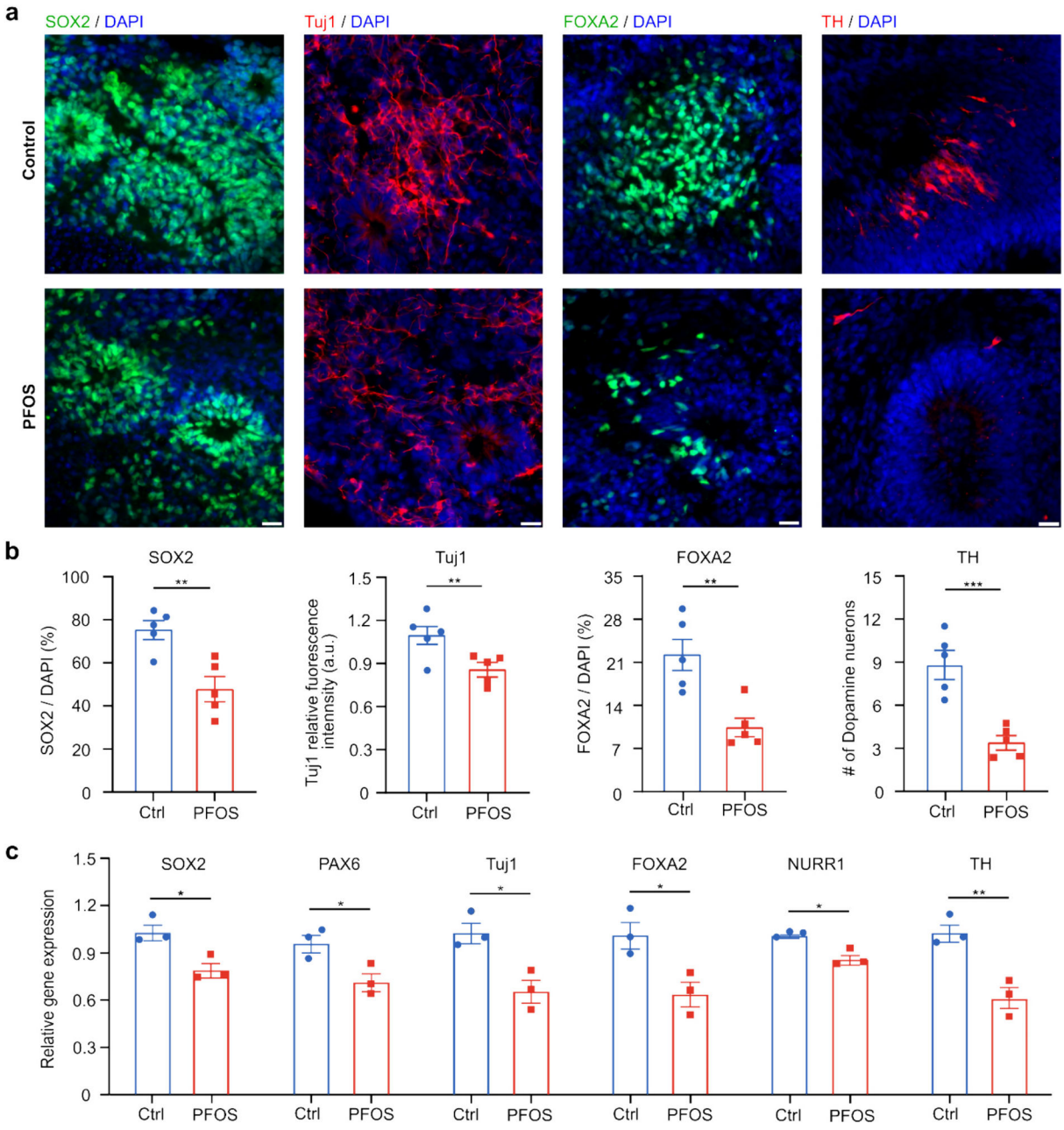

Fig. 3.

PFOS perturbs neural development. Immunofluorescence staining of neural progenitor cells (SOX2), early-stage neurons (Tuj1), midbrain floor plate progenitor cells (FOXA2) in one-month-old hMOs and dopaminergic neurons (TH) in two-month-old hMOs (a) and the corresponding quantification (b) after a 7-day exposure in the control (vehicle) and PFOS (300 μM) groups (mean ± s.e.m., unpaired t-test, n = 5 organoids, from 3 independent experiments). (c) qPCR analysis of relative gene expression of SOX2, PAX6, Tuj1, FOXA2, TH and NURR1 after a 7-day exposure in control group (vehicle treated with 0.05 % DMSO) and PFOS group (300 μM) (mean ± s.e.m., unpaired t-test, $n = 3$ organoids, from 3 independent experiments). Scale bar: 20 μm.

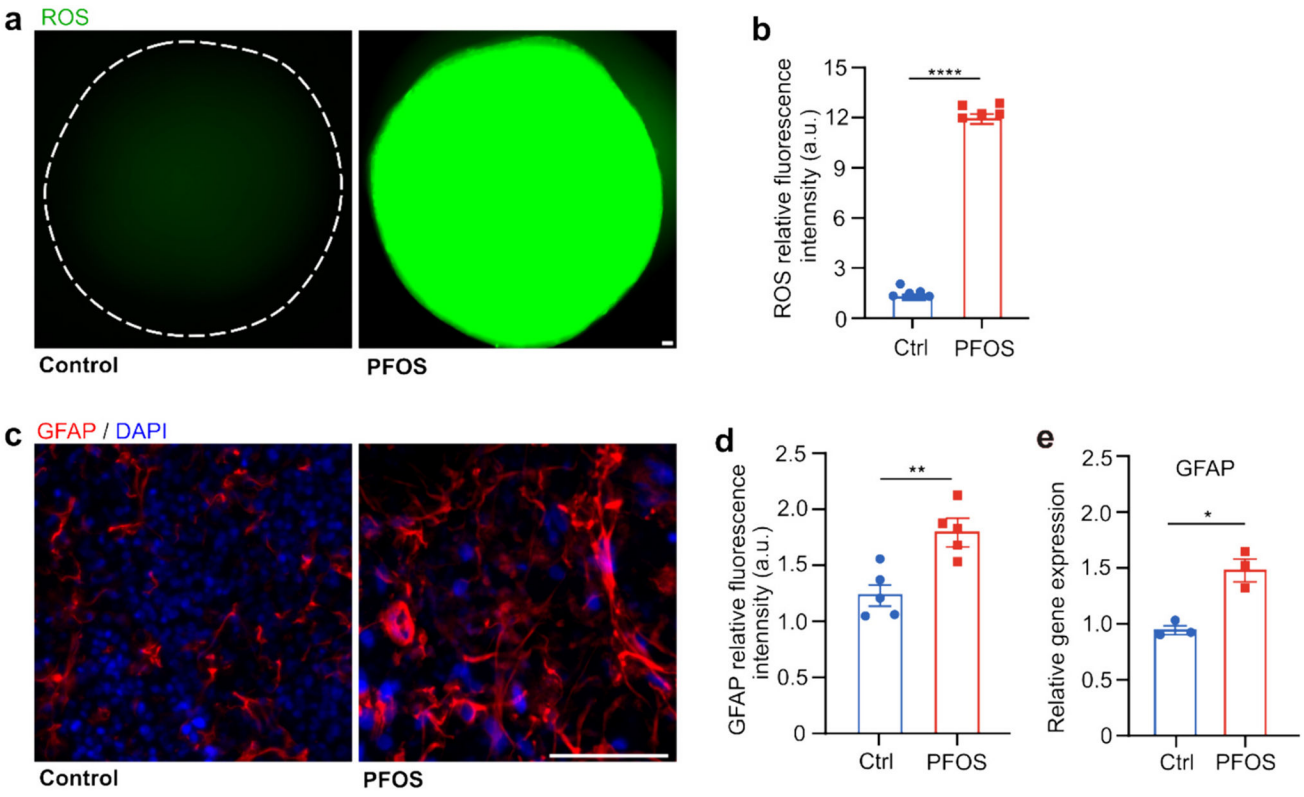

Fig. 4.

PFOS induces ROS generation and astrocyte activation. Fluorescent images of ROS indicator dye in two-month-old hMOs (a) and the corresponding quantification (b) after a 7-day exposure in control group (vehicle) and PFOS group (300 μM) (mean ± s.e.m., n = 5 organoids, unpaired t-test, from 3 independent experiments). Immunofluorescent staining of astrocytes (GFAP) in two-month-old hMOs (c), the corresponding quantification (mean ± s.e.m., unpaired t-test, n = 5 organoids, from 3 independent experiments) (d), and qPCR analysis of relative GFAP gene expression (e) after a 7-day exposure in control group (vehicle treated with 0.05 % DMSO) and PFOS group (300 μM) (mean ± s.e.m., unpaired t-test, n = 3 organoids, from 3 independent experiments). Scale bar: 50 μm.

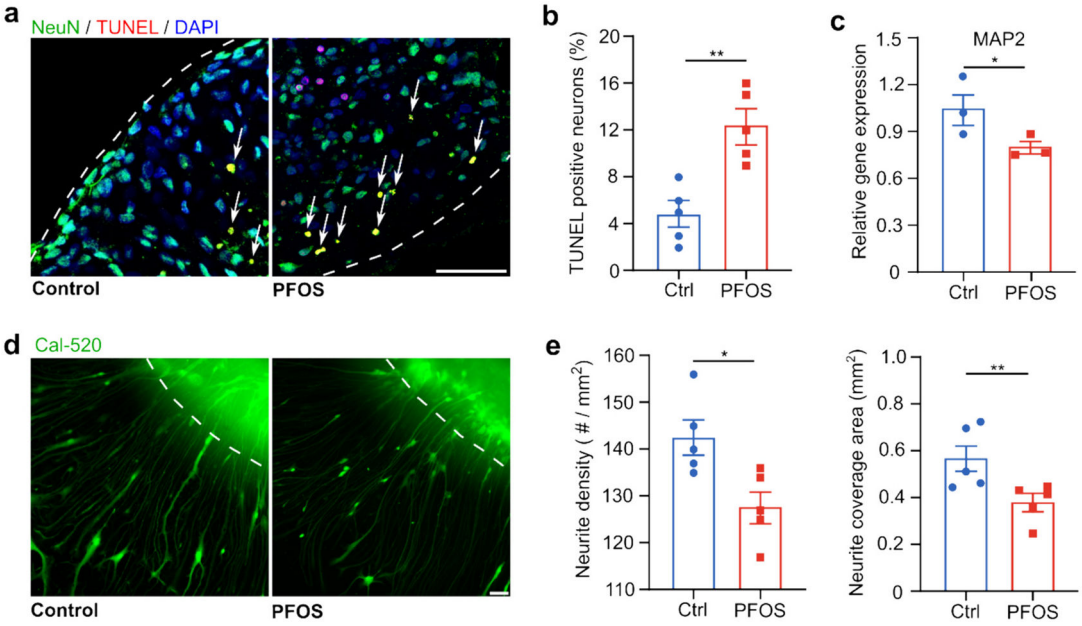

Fig. 5.

PFOS causes neuronal apoptosis and reduces neurite density. Immunofluorescent staining of neuronal apoptosis (TUNEL, NeuN, and DAPI) in two-month-old hMOs (a) and the corresponding quantification (b) after a 7-day exposure in control group (vehicle) and PFOS group (300 μM) (mean ± s.e.m., unpaired t-test, n = 5 organoids, from 3 independent experiments). (c) qPCR analysis of relative MAP2 gene expression after a 7-day exposure in control group (vehicle treated with 0.05 % DMSO) and PFOS group (300 μM) (mean ± s.e.m., unpaired t-test, n = 3 organoids, from 3 independent experiments). Fluorescent images of neurites of two-month-old hMOs (d) and quantification of neurite density and coverage area (e) after a 7-day exposure in control group (vehicle treated with 0.05 % DMSO) and PFOS group (300 μM) (mean ± s.e.m., unpaired t-test, n = 5 organoids, from 3 independent experiments). White dashed lines: the boundary of hMOs. Scale bar: 50 μm.